JOURNAL OF APPLIED POLYMER SCIENCE VOL. 21, 303–317 (1977)

Effect of Glass Reinforcement on Burning Rates of Poly(methyl Methacrylate) Composite Candles

JOEL W. BARLOW, *Department of Chemical Engineering, The University of Texas at Austin, Austin, Texas 78712*

Synopsis

Burning rates of glass-reinforced poly(methyl methacrylate) candles were measured under limiting conditions using an oxygen index apparatus modified to allow weighing of the candle as it burns. The limiting oxygen index was found to increase slightly with increasing concentration of glass in the candle for all samples tested. Burning rates were found to be a function of both glass concentration and orientation with respect to the propagating flame front. The burning rates of candles constructed from randomly oriented glass mats were found to increase with mat concentration by a factor of nearly 3 as mat content was increased to 70% by volume. The burning rates of candles constructed with unidirectionally oriented fibers, parallel to the flame propagation direction, were found to decrease by a factor of 2 as the glass concentration increased to 40% by volume. Erratic burning rates were observed for candles constructed with oriented fibers perpendicular to the flame propagation direction. These results are correlated by extension of existing thermally thin flame spread theories through consideration of composite solid-state energetics and the relative tendencies of the glass reinforcements to act as wicks for supplying the flame with degraded polymer liquid.

INTRODUCTION

The annual United States consumption of primarily glass fiber-reinforced plastics composites approaches 1 billion pounds, most of which is used in rather large-scale applications in the construction, transportation, and electrical industries.[1] Despite this large usage and the possible hazard it implies, very little has appeared in the open literature concerning the effects of glass fiber-reinforcement on the ignition and flame propagation characteristics of the composite structure.

The existing literature, though somewhat sketchy, indicates that the flammability characteristics of reinforced polymer systems are dependent on the nature, concentration, and orientation of the inert reinforcing phase as well as on the chemical nature of the polymer phase. For example, the introduction of inert fillers (glass fiber, alumina, and quartz) generally stabilizes the flame when the composite is burned in a candle-like mode. The presence of fillers may cause polymers which self extinguish through dripping to burn more intensely by preventing flow of the polymer away from the flame front.[2] The presence of noncombustible "ash" in the burning zone may also reduce flame propagation.[3] These apparently contradictory effects are generally dependent on the concentrations of fillers employed and on the type of polymer. The effects may also be dependent on the fibrous nature of the filler and on orientation of the fibers with respect to the advancing flame front. This seems to be the case with com-

posite systems used as reentry heat shields[4] for which it has been observed that fiber orientation perpendicular to the eroding and charring surface gives lower ablation rates and higher substrate temperatures than is achieved for other fiber orientations.[5] This effect is presumably caused by heat conduction and radiation along the fiber and is perhaps also operative in earth-bound fiber-reinforced composites subject to ordinary combustion conditions. In addition to the above physical phenomena, simultaneous DTA/TGA testing of composite systems has shown that normally inert fillers can increase pyrolysis rates and reduce ignition temperatures.[6,7] The degradation reactions caused by pyrolysis or oxidation are sometimes promoted by normally inert, incombustible materials with which the organic compounds are in contact.[6]

Given all these possibilities, it is not surprising that no general scheme for predicting the effects of fibrous fillers on the flammability of reinforced systems exists. No scheme is likely to emerge until a large number of systematic ignition and flame propagation experiments have been accomplished.

As a beginning effort in this regard, this paper reports some initial results obtained for candle-like burning of fiber glass-reinforced poly(methyl methacrylate) at close to limiting conditions. It is shown here that the physical nature of the glass reinforcement and its concentration strongly affect the rate of downward flame propagation as measured by the rate of mass loss in a modified L.O.I. apparatus. Further, it appears for this system that the flame propagation is controlled in part by the solid-state thermal energy mechanisms put forth by deRis[8] and McAlevy and co-workers.[9,10]

EXPERIMENTAL

Equipment

The basic equipment used is that recommended for the oxygen index flammability test developed by Fennimore and Martin[11] and further described by Isaacs[12] and ASTM Test Method D-2863-70. The test apparatus is widely used to determine the relative ease of ignition of polymeric systems and is both reliable and versatile. It is one of the few laboratory scale test methods which appear to be useful for predicting subsequent material performance in other laboratory scale tests.[13]

For the purpose of measuring burning rates, the basic oxygen index apparatus has been slightly modified by allowing the candle support rod to extend through the gas mixing bed to a load cell mounted below the apparatus. As shown in Figure 1, the modified apparatus consists of the standard 12-in. by 3-in.-I.D. Pyrex tube connected through flanges to a gas treatment section below. The gas treatment section, 7 in. by 3 in. I.D., is constructed of thin-walled stainless steel tubing. It is filled to a depth of 5 in. with $\frac{1}{16}$-in.-diameter ball bearings to evenly distribute the up-flowing gas mixture. Gas distribution is further aided by an annular manifold in the bottom of the section. Provision is made in this section for heating the incoming gas by use of two 500-watt band heaters clamped to the outside of the cylinder. The cylinder is insulated with $1\frac{1}{2}$ in. of asbestos lagging.

A $\frac{1}{2}$-in.-I.D. by 7-in. stainless steel tube is centrally located at the base of the heater section. Through this tube passes a 12-in. by $\frac{3}{8}$-in.-O.D. ceramic rod

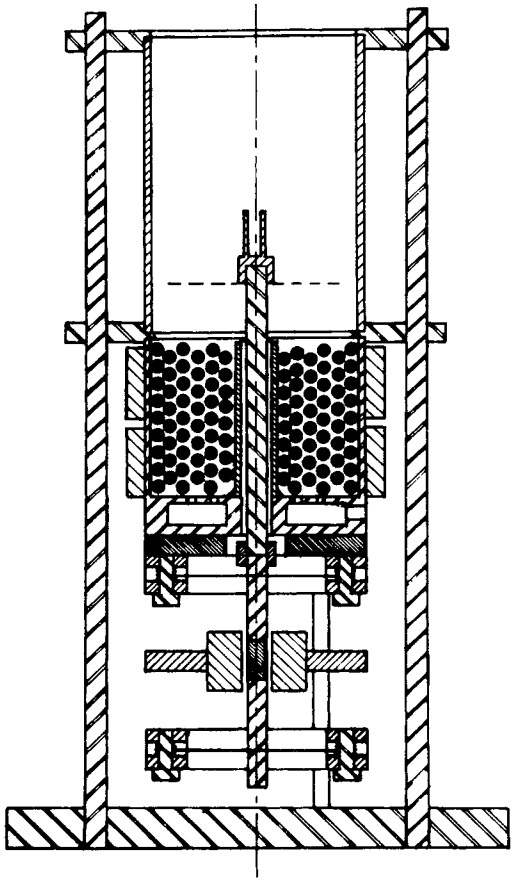

Fig. 1. Schematic of modified L.O.I. device.

which connects the polymer sample to the load cell. At its top end, the ceramic rod is fitted with a specimen clamp and a 1½-in.-diameter wire mesh screen which serves to catch any specimen fragments which may fall during burning. The lower end of the rod is connected by an aluminum sleeve to the load cell.

The load cell is separated from the gas conditioning section by a hollow, cylindrical pyrophylite block. The load cell, shown in detail in Figure 2, consists of a 6-in. by ¼-in.-O.D. aluminum rod which contains the iron core of a linear variable differential transformer (LVDT). The rod is held suspended at the centers of two support rings by 0.008-in.-diameter guitar strings which have been placed in tension by wire drives in the rings. Two wires pass through the rod at right angles in each wire support ring. This arrangement causes the aluminum and ceramic rod assembly to be fairly resistant to lateral displacements, thus avoiding the possibility of drag forces which could result if the sample support rod were to touch the steel tube surrounding it in the gas conditioning section. Small vertical loads on the suspended rod assembly, however, cause it to be easily and reversibly displaced.

Vertical core displacement is transformed into an electrical signal by the sensing coils of a Schaevitz 050HR LVDT which is positioned between the ring

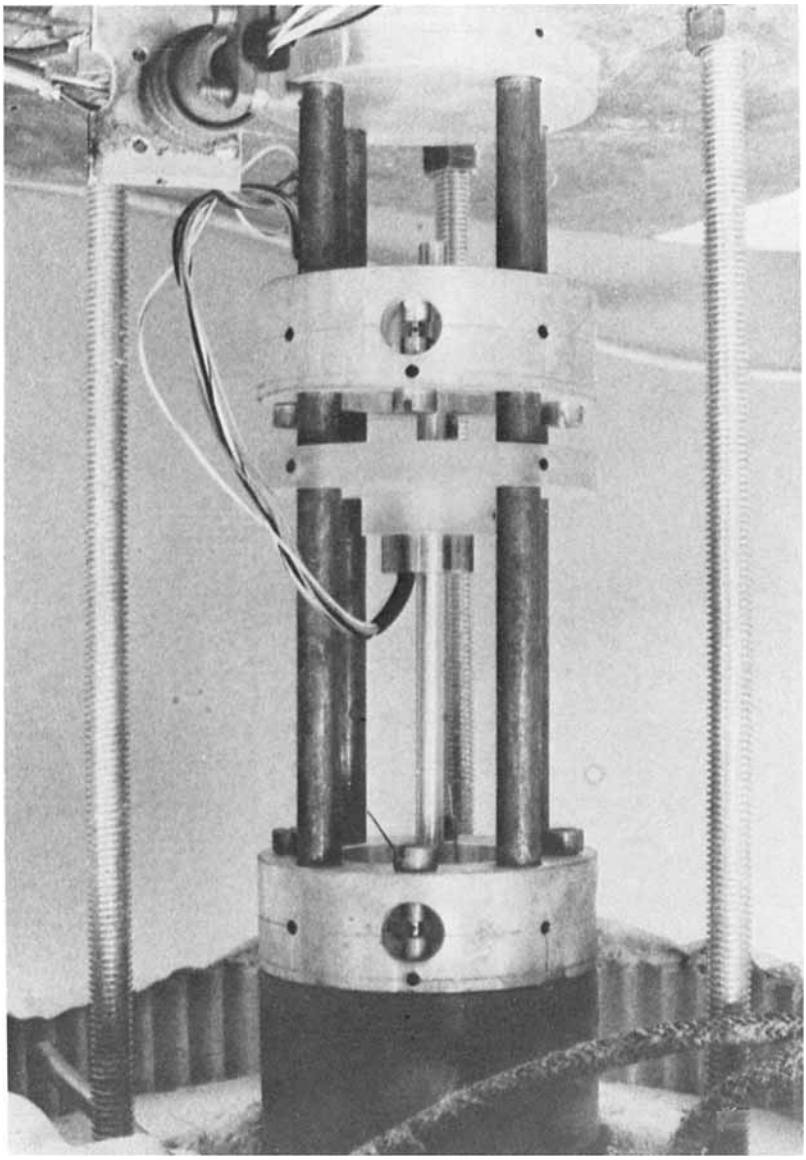

Fig. 2. Load cell details.

supports shown in Figure 2. The signal is amplified and conditioned by a Daytronic Model 830A module and recorded on a chart recorder.

The overall performance of the sample-weighing mechanism is quite good considering its simplicity. Load cell response to sample loads from zero to 3 g is very linear and rapid. With appropriate and frequent calibration, cell response is accurate to less than 1% relative error over the range.

Oxygen and nitrogen gas flow measurements are made in the usual way. Flow rates are measured using Fisher and Porter Models FP-1/4-16-6-5 and FP-3/8-25-5-6 rotameters on the oxygen and nitrogen lines, respectively. These meters are accurate to within 2% relative error. Combined gas flows, corrected for line

pressure drops, are maintained to give an upward velocity through the chamber of 4 ± 1 cm/sec at standard conditions in accordance with ASTM D-2863-70 for all tests reported here.

Sample Selection and Preparation

Fennimore and Jones[14] have experimentally shown that burning poly(methyl methacrylate) (PMMA) does not react chemically with the gas surrounding it, but merely vaporizes in the heat of the surrounding diffusion flames. They have also measured surface and flame temperatures and have estimated heat fluxes for candle-like burning of this material. Rohm and Haas PMMA is thus one of the few polymers whose burning has been characterized well enough to justify its use as a binder for studying the potentially more complicated case of candle-like burning of composite materials.

Two different types of glass mat were used in construction of the laminates. Unidirectionally oriented continuous fiber mats were prepared by winding glass roving on a slow-moving, 4-in.-diameter drum. During the winding operation, the fibers were coated with a 20% by weight PMMA in methyl ethyl ketone solution which, when dry, allowed removal of the mat from the drum without disturbing the fiber orientation. After removal, the cylindrical mat was softened with more solution, carefully flattened, and dried. The random glass mats used in this study were of the nonwoven form commonly used for hand lay-up construction. These mats were similarly treated with the PMMA solution to ensure good penetration of resin into the mat.

Composite laminates were prepared by interleafing the coated mats with thin sheets of PMMA such that the assembly was always faced with pure resin. The assemblies were then placed in a 7¼-in. × 7¼-in. × ⅛-in. aluminum mold and laminated at 200°C and 800 psi for about 30 min. During this process, excess resin was flashed from the mold to give a laminate approximately ⅛-in. thick with glass content largely controlled by the number of mats used in the construction.

All laminates were cut into 4-in. × ⅛-in. × ¼-in. candles for testing. The unidirectional laminates were cut so that candle-like burning would propagate parallel to the fibers (vertical fiber case) and at right angles to the fibers (cross fiber case).

The important thermal and physical properties of the laminate ingredients used are given in Table I. In addition, it was found that the thickness and density

TABLE I
Properties of Laminate Ingredients

Ingredient	ρ, g/cc	K, $\left(\frac{\text{cal}}{\text{cm sec °K}}\right) \times 10^4$	C, cal/g °K
PMMA[a]	1.185	5.0	0.35
Glass Roving	2.50[b]	26.0[c]	0.22[c]

[a] Average values taken from *Modern Plastics Encyclopedia*, 1961.

[b] Taken from G. S. Holister and C. Thomas, *Fiber Reinforced Materials*, Elsevier, New York, 1966.

[c] Taken from *Chemical Engineer's Handbook*, 4th ed., J. H. Perry, Ed., McGraw-Hill, New York, 1963.

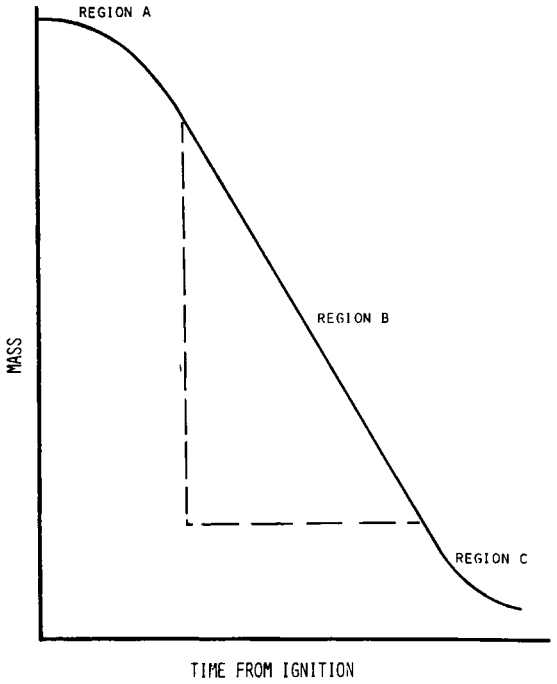

Fig. 3. Typical load cell response for candle-like burning of PMMA/glass composites.

of the commercial random glass mat used are important properties due to their control of propagation rates. The mats used in this study have a nominal thickness, measured by compression of the mat with a screw micrometer, of 0.017 in., a corresponding mat density of 1.109 g/cc, and a glass volume fraction of 0.4435.

Glass concentration in the laminates was determined by measurement of laminate densities owing to some difficulty in maintaining the ⅛-in. sample thickness as glass content increased. Glass concentration expressed as the volume fraction of glass in the composite structure, Φ_g, as computed by

$$\Phi_g = \frac{\rho_c - \rho_p}{\rho_g - \rho_p} \tag{1}$$

where ρ is the density and subscripts c, g, and p stand for composite, glass, and resin, respectively.

Test Procedure

The general features of the test procedure are exactly those outlined in ASTMD-2863-70. First, the limiting oxygen index of each composition is found using the ASTM 3-min burning criterion. The oxygen partial pressure is then increased by approximately 0.002 and the burning rate measured.

A typical recorder output of weight loss versus time is shown in Figure 3. The sample begins to burn slowly after ignition (region A), then the rate accelerates to a steady-state rate (region B). As the downward propagating flame front

approaches the sample clamp, the burning rate again decreases (region C). The burning rate is easily computed from the slope of steady-state region B.

Generally, five separate determinations are made of burning rates for each composition. The results reported in the following sections represent the average of these five determinations. The oxygen partial pressures reported are those corresponding to the burning rate determinations. All tests were performed at ambient temperature conditions. Gas preheating was not employed.

RESULTS AND DISCUSSION

The results of burning random mat- and oriented mat-reinforced PMMA at conditions close to limiting are shown in Table II. The limiting oxygen index obtained for all the samples is somewhere between 14.6 and 15.3, depending on the glass concentration. This range is somewhat lower than the value 17.3 ± 0.1 reported by Fennimore and Martin.[11] The precise reason for this discrepancy is not clear, but is likely due to inaccuracies in the flowmeters and possibly to aerodynamic effects resulting from the modifications in design discussed earlier.

For all cases, a slight trend of increasing limiting oxygen concentration with increasing glass content is seen. This trend is expected on the basis of the increasing difficulty of ignition as the material density and thermal conductivity increases through increased glass content.[15] Considering that flame propagation is a continuing ignition process, one might expect that the burning rate, as measured by rate of mass loss, would similarly decrease as glass content increased at constant oxygen pressure or at least that it would stay relatively constant for all burning at limiting conditions. The results in Table II, however, indicate that the burning rate may increase, decrease, or become erratic, depending on

TABLE II
Mass Loss Rates for Candle-Like Burning of Glass Fiber/PMMA Laminates

Sample designation	Oxygen index n[a]	Glass vol. fraction Φ_g	Rate, g/min
Random mat	14.6	.030	.075 ± .005
	14.7	.060	.075 ± .008
	14.9	.144	.108 ± .010
	14.8	.146	.107 ± .005
	14.9	.167	.140 ± .010
	14.9	.180	.130 ± .008
	15.3	.231	.140 ± .015
	15.3	.296	.184 ± .008
Continuous vertical fiber	14.7	.098	.023 ± .002
	15.1	.131	.020 ± .002
	15.1	.155	.019 ± .004
	15.1	.210	.0165 ± .002
	15.1	.417	.0130 ± .002
Continuous cross fiber	14.5	.098	.07–.151
	14.5	.231	.077–.138
	14.7	.300	.130–.190
	15.1	.300	.105–.278
	15.3	.300	.120–.200

[a] $n = \dfrac{[O_2]}{[O_2] + [N_2]} \times 100 = P_{O_2} \times 100$, where P_{O_2} is the O_2 partial pressure.

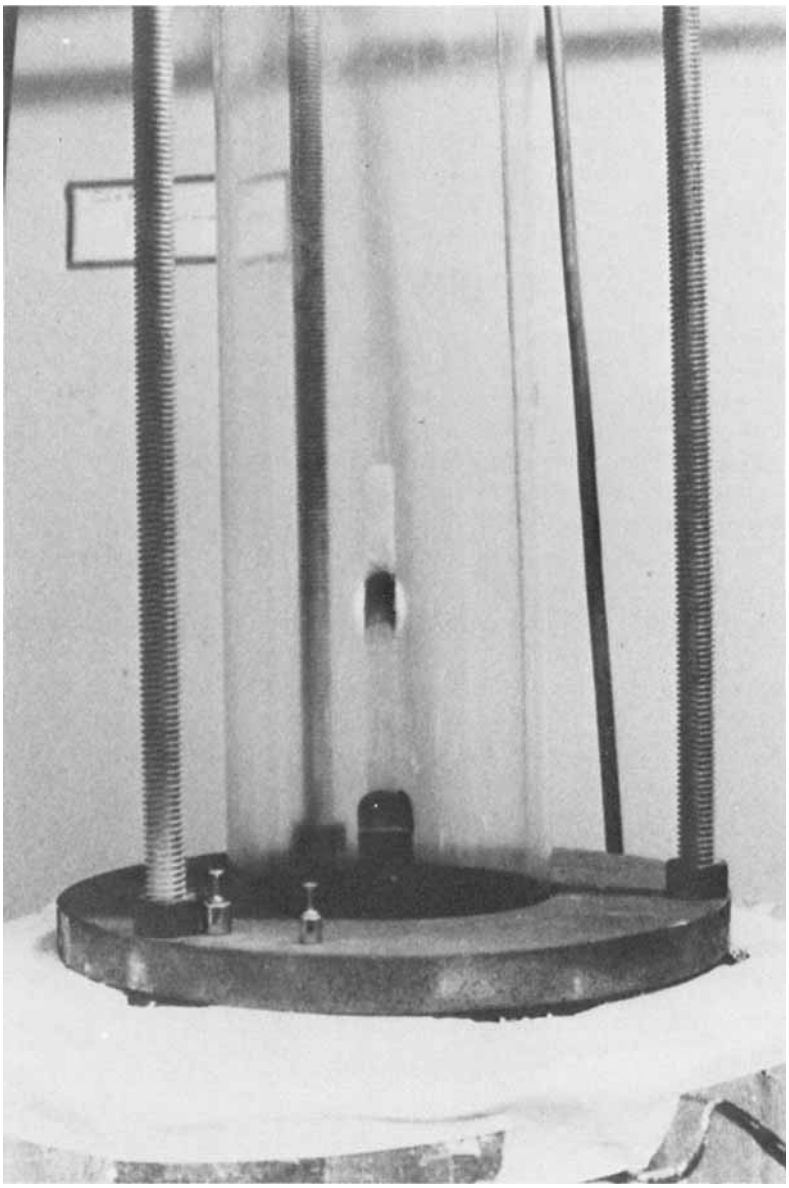

Fig. 4. Typical burning behavior of a random mat-reinforced candle.

the nature of the reinforcement and its orientation with respect to the downward-propagating flame front.

A photograph of a typical burn of a candle constructed with random glass mat is shown in Figure 4. Here the major features of the burning process are seen clearly. The forward edge of the downward-propagating flame front is extended slightly ahead of what appears to be a pyrolysis zone in the interior of the flame in which carbon is produced. This carbon layer is oxidized at the top of the buoyant flame leaving a clean, mechanically stable glass "ash." Candles constructed on continuous vertical fibers which remain well anchored as the flame

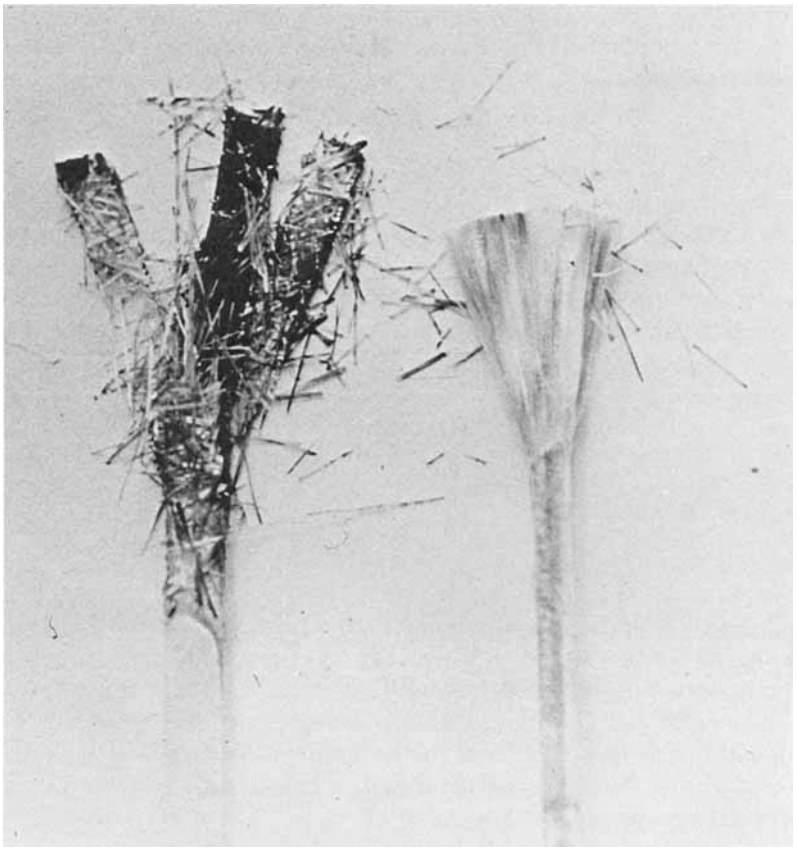

Fig. 5. Ash configurations for random mat (left) and continuous vertical fiber reinforced (right) candles. Random mat ash is separated to show ply geometry.

propagates downward show similar zones of behavior, although the "ash" has a considerably different physical character, as shown in Figure 5. Candles constructed with horizontal fibers, on the other hand, do not produce a mechanically stable "ash." Rather, as the flame front passes, the horizontal fibers become dislodged and either curl into the flame or flake off to be caught by the screen below the candle holder. It appears that curling of fibers into the flame tends to inhibit burning of the candle, often slowing the burning rate to the point of extinction. Flaking off, on the other hand, tends to generate new polymer surfaces in the flame interior, which results in the sample burning more strongly. This phenomenon is apparently what causes the very erratic burning rates observed for candles reinforced with horizontal fibers in Table II. Thus, consistency of burning behavior seems to be a function of the mechanical stability of the "ash."

A comparison of the stable ashes shown in Figure 5 with the corresponding differences in burning rates of random mat- and continuous fiber-reinforced candles in Table II further leads to the tentative conclusion that the geometric configuration of the mechanically stable fibers also strongly affects the burning rate of the composite with random glass mat construction, causing the burning rate to increase with increasing glass content, while increasing the content of

vertical fibers decreases the burning rate. A partial explanation of this phenomenon can be obtained by extension of existing flame spread theories to handle composite materials.

Extension of General Theories

The very similar theories put forth by deRis[8] and Lastrina and co-workers[9,10] for prediction of flame spread velocities over fuel beds have proved quite successful. In these theories, it is postulated that the process controlling the flame spread phenomena occur in a very small ignition region δ at the leading edge of the spreading flame, adjacent to the surface. Their solutions of the combined solid-phase energy and gas-phase conservation equations lead to the following simplified expressions:[9,10]

Thin fuel bed ($\bar{\tau} < 1$)

$$V' \simeq \frac{q\delta}{\rho_s C_s \tau'(T_b - T_0)} \tag{2}$$

Thick fuel bed ($\bar{\tau} > 1$)

$$V \simeq \frac{q^2\delta(1.272)}{K_s \rho_s C_s (T_b - T_0)^2} \tag{3}$$

where V and V' are the spreading flame velocities; q is the heat flux to the fuel surface in the ignition region; ρ_s, C_s, and K_s are the solid density, heat capacity, and thermal conductivity, respectively; T_b is the surface temperature of the fuel in the burning region; T_0 is the fuel temperature a large distance from the burning region; and τ' is the distance from the burning fuel surface into the bulk of the fuel at which the thermal gradient is zero. The factor $\bar{\tau}$ is a nondimensional critical thickness parameter computed by

$$\bar{\tau} = \tau' \sqrt{\frac{V}{\alpha_s \delta}} \tag{4}$$

where α_s is the thermal diffusivity of the solid, $K_s/\rho_s C_s$, which expresses the extent to which subsurface thermal gradients are important to the flame spreading process.

Equation (3), the thermally thick solution, has been successfully applied by Funt and Magill[16] to correlation of propagation velocities in the range of 8 to 70 in. per minute for thin polystyrene films burned in enriched oxygen atmospheres (n = 20–50%). Similar velocity measurements for PMMA have been correlated with eq. (3) for horizontal propagation in environments with superambient polymer temperatures and oxygen concentrations.[17]

It is not altogether clear, however, that eq. (3) is necessarily appropriate for downward flame propagation in general. For example, Parker[18] concluded that for thin cellulose cards, the pyrolysis zone occurs beneath the flame rather than ahead of it, and that extension of the flame beyond the pyrolysis zone due to gaseous diffusion preheats the surface to the pyrolysis temperature by gas-phase heat conduction, thus controlling propagation of the flame. If this situation occurs, then the subsurface gradients are less important and eq. (2) is more appropriate. Using these observations, Campbell[19] has used eq. (2) to correlate downward propagation velocities for cellulose sheets, with good results.

Careful examination of Figure 4, likewise, shows that the flame front extends below the zone of degradation so that the mechanism proposed by Parker and

Campbell is likely to occur in the polymer composite systems reported here. An additional check on the validity of a thermally thin model for PMMA candles can be made using eqs. (2)–(4) and the experimental data reported by Fennimore and Jones.[14] They report the equivalent of a 2.6×10^{-3} cm/sec downward propagation velocity for the burning of ¼-in.-diameter rods in a 20% O_2 environment, and they further report that the flux to the polymer surface is 0.5 cal/cm^2-sec and that the polymer surface temperature under the flame is 850°K. Inserting these numbers into eqs. (2) and (3) along with physical property values from Table I yields ignition zone dimensions δ of 0.37 and 0.72 cm, respectively, for τ' equal half the sample diameter and T_0 equal to 300°K. The corresponding critical thickness parameter values from eq. (4) are then 0.75 and 0.54 for the thin and thick cases, respectively, and the candles reported by Fennimore and Jones are, therefore, thermally thin. Similar calculations to those above, using the data reported in Table II, indicate that all of the samples reported herein behave in a thermally thin manner. Thus, eq. (2) is the appropriate equation to generalize for modeling the behavior of the composites burned according to the reported conditions.

Assuming that both reinforced and nonreinforced specimens are burned under identical circumstances and that the glass reinforcement in no way affects q, δ, or T_b, one is led by eq. (2) to the following ratio of propagation velocities:

$$\frac{V'_c}{V'_p} = \frac{\rho_p C_p}{\rho_c C_c}\left(\frac{\tau'_p}{\tau'_c}\right) = \frac{\rho_p C_p}{\rho_c C_c}\left(\frac{t_p}{t_c}\right) \tag{5}$$

where subscript c refers to the laminate composite and p to the pure polymer, and τ' is assumed to be half the sample thickness t. The specific heat of the composite may be written in terms of the mass fraction average of the specific heats of its components

$$C_c = W_g C_g + W_p C_p \tag{6}$$

where W_i is the mass fraction of component i. Recognizing that the mass fraction is related to the volume fraction through the relationship $\Phi_i = W_i \rho_c / \rho_i$, eq. (6) may be rewritten as

$$C_c = \frac{C_p \rho_p \Phi_p}{\rho_c}\left[1 + \frac{\rho_g C_g}{\rho_p C_p}\frac{\Phi_g}{\Phi_p}\right] \tag{7}$$

The rate of mass loss for a composite composed of inert fibers is related to the propagation velocity and the area fraction or volume fraction of polymer, Φ_p, via

$$\dot{m}_c = V'_c \rho_p \Phi_p A_c \tag{8}$$

where A_c is the area of the specimen affected as the flame front moves through. The mass loss of the pure polymer burning in a comparable manner is just

$$\dot{m}_p = V'_p \rho_p A_p \tag{9}$$

Combining eqs. (5), (7), (8), and (9) yields

$$\frac{\dot{m}_c}{\dot{m}_p} = \frac{t_p}{t_c} \cdot \frac{1}{1 + \dfrac{C_g \rho_g}{C_p \rho_p}\dfrac{\Phi_g}{\Phi_p}} \cdot \frac{A_c}{A_p} \tag{10}$$

as the general expression for the expected ratio of mass loss rates for composite and pure polymer candles burned under identical circumstances. Identifying the areas A_c and A_p with the cross-sectional areas of the composite and polymer candles allows one to write a ratio of mass fluxes through the cross sections.

$$\frac{N_c}{N_p} = \frac{t_p}{t_c} \frac{1}{1 + \dfrac{C_g \rho_g}{C_p \rho_p} \dfrac{\Phi_g}{\Phi_p}} \tag{11}$$

where $N_i = \dot{m}_i / A_i$. This expression will prove useful in subsequent discussions.

Random Mat Composites

Since the ratio $(C_g \rho_g / C_p \rho_p)$ is 1.15 from Table I, eq. (10) predicts that the mass loss ratio should decrease as the glass content increases for all glass-reinforced systems whose thicknesses are comparable to those of the pure polymer. The data in Table II, however, show that the rate of mass loss increases with increasing glass content from a zero glass value of 0.065 g/min (extrapolated) to over 0.18 g/min at a glass content of 30% by volume.

One explanation of this effect is based on noting that the random mat plies retain their individual integrities during the burning process as shown in Figure 5. Also, these plies are observed to exert substantial wicking when burning insofar as no dripping of molten polymer is observed at glass concentrations greater than 10% by volume. These observations lead one to expect that the flame propagation velocity is controlled by the properties of the random glass mat wicks in the system.

Provided that only the solid-state properties of the wick are important, that is, provided the area for heat and mass transfer with the flame and the gas phase properties are the same for wick burning and pure polymer candle burning, eq. (11) can be used to predict the mass flux ratio for a single random wick. As noted earlier, the random mats have a nominal thickness of 0.017 in. and a glass volume fraction of 0.4435. The pure polymer candles used to establish $\dot{m}_p$ have a nominal thickness of 0.125 in. Substitution of these numbers into eq. (11) yields $N_w/N_p = 3.597$ as the ratio of the mass flux for a single ply, N_w, to that existing for a pure polymer candle, N_p, burned under identical conditions.

The composite laminate is composed of several mat wicks and, provided these wicks are noninteracting, the overall burning rate of the laminate could be expected to be proportional to the number of wicks in the system. Assuming that these wicks exert a fairly localized influence in the degradation zone, some polymer in the laminate structure could be expected to degrade and burn in the usual manner. The total mass rate of degraded polymer into the flame under these circumstances is then

$$\dot{m}_c = N_p A_p + N_w A_w = \langle N \rangle A \tag{12}$$

where A_p and A_w represent the cross-sectional areas of pure polymer and plies in the composite laminate which has a total crosssectional area $A = A_p + A_w$.

For pure polymer candles with total cross sections A identical to those of the laminate candles, we have

$$\dot{m}_p = N_p A \tag{13}$$

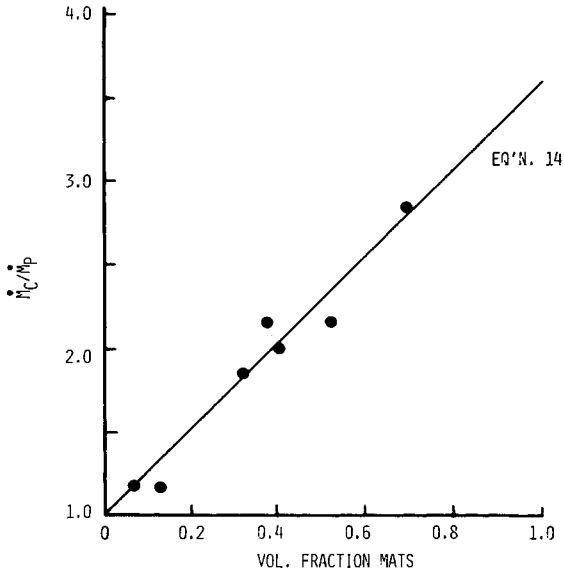

Fig. 6. Comparison of predicted and observed burning rate ratios for random mat-reinforced PMMA candles.

Combining eqs. (12) and (13) then yields

$$\frac{\dot{m}_c}{\dot{m}_p} = \frac{A_p}{A} + \frac{N_w A_w}{N_p A} \tag{14}$$

$$= \Phi_w \left(\frac{N_w}{N_p} - 1 \right) + 1$$

$$= 2.597 \Phi_w + 1$$

where Φ_w is the area fraction, or equivalently the volume fraction, of random mats in the composite laminate and is related to the total glass content of the composite by $\Phi_w = \Phi_g / \Phi_{gm}$; Φ_{gm} is the glass content of the mat, 0.4435 in our particular case.

Figure 6 shows that the agreement between eq. (14) and the experimentally observed ratios computed from the values in Table II, using $\dot{m}_p = 0.065$ g/min, is excellent and seems to justify all of the assumptions leading to the equation. The value of $\dot{m}_p$ is obtained by extrapolation of the random mat data, Table II, to zero glass concentration and is presumably a measure of the rate of degradation of pure polymer. This value appears to be in good agreement with that reported by Fennimore and Jones[14] for burning of pure polymer candles.

Continuous Vertical Fiber Laminates

By contrast to behavior of random mat laminates, continuous vertical fiber laminates do not wick very well when burned as candles. Instead, at fiber volume fractions below 0.2, a molten polymer front tends to flow down the outside of the candle in advance of the propagating flame. Presumably this is, in part, caused by the lack of cross fibers which would tend to slow the flow from the molten zone

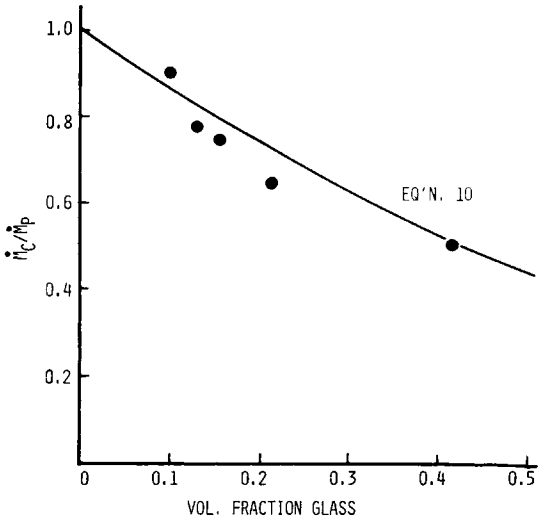

Fig. 7. Comparison of observed burning rate ratios with prediction for unidirectional, vertical glass fiber-reinforced PMMA candles.

and promote wicking. Examination of Figure 5 shows, further, that there is no particular mat definition or characteristic mat thickness, particularly in samples containing large volume fractions of glass. Instead, the glass tends to "bush out," giving the appearance of a paint brush, as the flame front passes.

Lack of wicking and definable mat geometry would seem to imply that eq. (10) could be applied directly to the prediction of the decrease of the mass loss rate of the composite with increasing glass content by setting $\tau'_p = \tau'_c$ and $A_c = A_p$ for pure and reinforced candles with equivalent geometry. Figure 7 shows the comparison of eq. (10) and the experimental data of Table II. Again, the fit to data looks fairly reasonable, indicating that the thermally thin model is appropriate for predicting the changes in propagation velocity with glass content. The value of $\dot{m}_p$ required to obtain this fit, however, is only 0.0255 g/min, a value that is considerably lower than the 0.065 g/min observed for the random mat case.

SUMMARY AND CONCLUSIONS

It appears that candle-like burning rates of glass-reinforced PMMA at conditions close to limiting can be partially predicted from solid-state energy considerations through extension of existing flame spread models. If the configuration of the glass reinforcement is such that a stable glass ash capable of promoting wicking of the degraded polymer liquid occurs, the observed increase in burning rate with glass content can be correlated from knowledge of the wick geometry and concentration in the composite candle. The decrease in candle burning rates with increase in concentration of unidirectional glass fibers oriented parallel to the downward propagating flame front can also be adequately correlated.

Despite the adequacy of the models presented for correlating the changes observed in burning rates with glass type and content, it does not appear possible to directly predict composite burning rates from consideration of pure PMMA burning rates and the glass reinforcement. The burning rate of pure PMMA

is not well defined primarily due to its tendency to drip excessively when burning, a situation which leads to erratic and abnormally low mass loss rates as measured by this test. The values of $\dot{m}_p$ obtained by extrapolation of reinforced candle data to zero glass content are seen to be substantially different and a function of the type of reinforcement used. This theoretically unjustified situation seems to reflect the ability of the reinforcement to prevent flow of the polymer liquid away from the combustion zone insofar as reinforcements with cross fibers yield higher extrapolated pure polymer burning rates than those without. Formulation of a truly predictive model of flame propagation rates for composite systems composed of polymers which degrade to low-viscosity liquids will require consideration of this rheological problem.

Provided one experimentally determined burning rate at conditions close to limiting is available, for a fiber-reinforced polymer candle which degrades to liquid and stable ash, the flame spread models presented above appear adequate for estimating burning rates at other fiber concentrations. Caution should be used, however, when applying these models to composites and conditions dissimilar to those outlined above. Burning composite candles under enriched oxygen conditions may lead to thermally thick propagation behavior, and use of polymers which degrade to char instead of liquids may lead to quite different results. These considerations must be the object of further study if a complete understanding of composite burning rates is to be obtained.

This work was supported by E. I. Du Pont de Nemours and Company through its Young Faculties Grant program with The University of Texas at Austin Department of Chemical Engineering. This support is greatly appreciated. The careful work of Mr. L. Bannon, an undergraduate research assistant whose measurements comprise the bulk of this paper, is also acknowledged.

References

1. *Mod. Plast.* 36 (Jan. 1974).
2. E. V. Gouinlock, J. F. Porter, and R. R. Hindersinn, *J. Fire Flamm.*, **2**, 206 (1971).
3. F. J. Martin and K. R. Price, *J. Appl. Polym. Sci.*, **12**, 143 (1968).
4. J. Malott, *SPE J.*, **17** (5), 449 (1961).
5. E. Baer, *Engineering Design for Plastics*, Reinhold, New York, 1964, p. 852.
6. A. W. Benbow and C. F. Cullis, paper presented at Central states and Western States Section, The Combustion Institute, San Antonio, Texas, Meeting Apr. 21–22, 1975.
7. C. Z. Carroll-Porczynski, *Composites* 4(1), 9 (1973).
8. J. N. deRis, Proceedings 12th Symposium (International) on Combustion, Univ. Poitiers, France, The Combustion Institute, 1969, p. 241.
9. R. F. McAlevy and R. S. Magee, Proceedings 12th Symposium (International) on Combustion, Univ. Poitiers, France, The Combustion Institute, 1969, p. 215.
10. F. A. Lastrina, R. S. Magee, and R. F. McAlevy, Proceedings 13th Symposium (International) on Combustion, Univ. Utah, Salt Lake City, The Combustion Institute, 1971, p. 935.
11. C. P. Fenimore and F. J. Martin, *Mod. Plast.*, **43**, 141 (Nov. 1966).
12. J. L. Isaacs, General Electric TIS Report 69-MAL13, Louisville, Ky., August 1969.
13. M. A. Harpold and K. E. Atkins, *J. Fire Flamm.*, **4**, 2 (1973).
14. C. P. Fennimore and G. W. Jones, *Combustion and Flame*, **10**, 296 (1966).
15. C. J. Hilado, *J. Cell. Plast.* 181 (1971).
16. J. M. Funt, and J. H. Magill, *J. Fire Flamm.*, **4**, 174 (1973).
17. R. S. Magee and R. F. McAlevy III, *J. Fire Flamm.*, **2**, 271 (1971).
18. W. J. Parker, *J. Fire Flamm.*, **3**, 254 (1972).
19. A. S. Campbell, *J. Fire Flamm.*, **5**, 167 (1974).

Received August 21, 1975
Revised January 13, 1976